Available online at www.sciencedirect.com
SCIENCE DIRECT
Journal of Catalysis 230 (2005) 38–51
JOURNAL OF CATALYSIS
www.elsevier.com/locate/jcat

Mechanism of *n*-butene skeletal isomerization over HFER zeolites: a new proposal

B. de Ménorval, P. Ayrault, N.S. Gnep, M. Guisnet *

Laboratoire de Catalyse en Chimie Organique, Université de Poitiers, UMR 6503, Faculté des Sciences, 40 avenue du recteur Pineau, 86022 Poitiers cedex, France

Received 9 July 2004; revised 21 September 2004; accepted 22 September 2004

Available online 28 December 2004

Abstract

The effect of time on stream (from 1 min to 44 h) on the rate and selectivity of *n*-butene isomerization and on the concentration of protonic sites interacting with ammonia or deuteroacetonitrile was determined over a HFER zeolite with a Si/Al ratio of 10. Aging for 44 h was shown to increase the selectivity from 55 to 95% and the turnover frequency for isomerization from ~ 250 to 4000 h^{-1}. All of this can be explained by considering the HFER pore system as equivalent to a series of noninterconnected nanoreactors (the 10-membered ring channels) into which the reactant molecules have to diffuse without any possibility of desorption before their exit while undergoing various successive bimolecular reactions. In nanoreactors with few protonic sites, *n*-butene isomerizes selectively through an autocatalytic process; in those with many sites a thermodynamic equilibrium mixture of propene, butenes, pentenes, and deactivating carbonaceous species is formed.

Keywords: HFER zeolite; *n*-Butene skeletal isomerization; Mechanisms; Turnover frequency; Shape selectivity

1. Introduction

HFER, the protonic form of the ferrierite zeolite, was shown to be a highly selective and stable catalyst for the skeletal isomerization of *n*-butenes into isobutene at relatively low temperatures (~ 350 °C) [1–3]. However, the initial selectivity for isobutene is generally low, with a simultaneous production of propene, pentenes, and isobutene. This is typical of a bimolecular transformation of *n*-butenes involving, successively, *n*-butene dimerization (D), isomerization (I), and cracking (C) of octenes (Scheme 1) [3–5].

All of the steps of this pathway are known to be very facile. Thus dimerization D (actually oligomerization) of 1-butene was shown to occur very quickly at room temperature and even lower temperatures over protonated zeolites [6]. Cracking of octenes (C), which involves the same steps as dimerization but in the reverse order, is also very facile to catalyze. This is also the case for the skeletal isomerization of alkenes with more than four carbon atoms, which can occur at relatively low temperatures on weak protonic acid solids such as Al_2O_3 [7,8].

A decrease in the activity of HFER and a significant increase in selectivity for isobutene can be observed with increasing time on stream (TOS). Both were associated with the retention of heavy secondary products within zeolite micropores [3–5,9–21]. These products (called "coke") caused a significant blockage of the access to the micropores [11–14,16–23] and deactivation of most of the protonic sites [4,18–20,23]. Coke was found to be constituted of slightly condensed aromatic molecules (containing two to four aromatic rings) with methyl substituents [23]. Monte Carlo docking showed that most of the coke molecules were preferentially

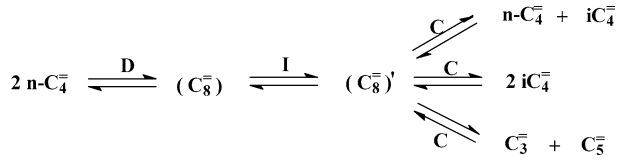

Scheme 1.

* Corresponding author.
E-mail address: michel.guisnet@univ-poitiers.fr (M. Guisnet).

0021-9517/$ – see front matter
doi:10.1016/j.jcat.2004.09.021

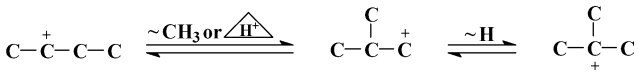

Scheme 2.

sited within one or two intersections of 10- and 8-membered ring (MR) channels along the 10-MR channels [24].

Experiments carried out with *n*-butene containing one ^{13}C atom [16,25,26] show large differences in the composition of isobutene formed on fresh and aged samples: 25% of the molecules had no ^{13}C, 25% had two ^{13}C atoms, and 50% had one ^{13}C atom in the former case and more than 90% contained only one ^{13}C atom in the latter. The distribution found on fresh HFER samples is that expected from the bimolecular pathway described in Scheme 1, in which cracking (steps C) would occur from octene intermediates with a random distribution of ^{13}C atoms [16,25]. On the other hand, the isotopic distribution of isobutene molecules over aged HFER samples and their high selectivity for isobutene are in agreement with a monomolecular mechanism. Therefore, the increase in selectivity with TOS has often been explained by the coexistence of mono- and bimolecular pathways over nonselective fresh zeolite; of these, the bimolecular pathway has a much higher sensitivity to deactivation by coke.

However, there is a major objection to this simple proposal: the monomolecular acid-catalyzed formation of isobutene involves a highly unfavorable primary isobutyl carbenium ion (Scheme 2).

Therefore, a significant effort has been made to justify the existence of such transition states in zeolites [10,27,28]. However, the monomolecular reaction should not be faster than the bimolecular process, which involves only facile steps with protonated cyclopropane, and secondary and tertiary carbenium ions as transition states [5]. The very low rate of the monomolecular isomerization pathway was further demonstrated in *n*-butane isomerization both in superacidic media [29] and over bifunctional Pt/silica alumina catalysts [30]. Under conditions where *n*-pentane and *n*-hexane were rapidly isomerized, the transformation of *n*-butane into isobutane was very slow; moreover, the rearrangement of 1-^{13}C-*n*-butane into 2-^{13}C-*n*-butane (the scrambling reaction), which involves the same steps as *n*-pentane and *n*-hexane isomerization, occurred at a similar rate.

Therefore, if the monomolecular isomerization pathway is really predominant over the aged HFER samples, it can be expected that the activity of the acidic sites (i.e., their turnover frequency, TOF) will be at least lower (normally much lower) than the TOF of the fresh HFER samples on which isobutene essentially results from a bimolecular mechanism. Up to now, no comparison between the TOF values of fresh and aged HFER has been reported in the literature. However, in recent papers, van Donk et al. [18,20] have shown the large effect of coke on the residual acidity of HFER samples. Thus, after 20 h on stream (6.4 wt% C), only 5% of the bridging OH groups (which are the protonic acid sites) of a HFER sample with a Si/Al ratio of 30 were found to be free; furthermore, the intensity of the IR band at 2292 cm^{-1} (which corresponds to deuterated acetonitrile coordinated to Brønsted acid sites) on a sample of the same zeolite aged for 200 h (6.8 wt% C) was 7 times lower than on fresh HFER. Unfortunately, the activity of the fresh HFER was not determined and the comparison of TOF values was limited to samples aged for different times [20].

In this paper, the effect of TOS (from 1 min to 44 h) on the rate and selectivity of *n*-butene transformation at 350 °C over a HFER sample with a Si/Al ratio of 10 was determined. To obtain accurate values for rate, *n*-butene transformation was carried out at four different contact times. HFER samples aged for different times, and hence with different coke contents, were characterized by nitrogen and *n*-butane adsorption and by ammonia and deuteroacetonitrile adsorption followed by IR spectroscopy. The TOF values for the formation of the primary products were estimated from the values of rates and of concentration of the protonic acid sites of the HFER samples. It is shown that the TOF value for the skeletal isomerization of *n*-butene was 10 to 40 times greater on HFER aged for 44 h (8.1 wt% C) than on fresh HFER. This allows us to reject the proposal of a classical monomolecular process for *n*-butene isomerization over aged HFER samples. A new proposal is advanced that explains the effect of aging of HFER and the effects of the Si/Al ratio and the partial pressure of *n*-butene on the selectivity for isobutene.

2. Experimental

The ferrierite sample (total Si/Al ratio of 10.2), supplied in its ammonium form by Zeolyst International, was calcined under dry air flow (60 $ml\,min^{-1}\,g^{-1}$) for 10 h at 500 °C to obtain the protonic form (HFER). The fresh HFER sample displayed a concentration of protonic sites of ~ 0.9 $mmol\,g^{-1}$, determined from the intensity of the IR NH_4^+ band at 1458 cm^{-1}. Nitrogen physisorption/*t*-plot analysis showed a micropore volume of 0.154 $cm^3\,g^{-1}$ and an external surface area of 18 $m^2\,g^{-1}$.

The transformation of 1-butene was carried out in a fixed-bed reactor under the following conditions: 350 °C, atmospheric pressure, a N_2/butene molar ratio of 9, a weight hour space velocity (WHSV) of 13, 20, 60, and 120 h^{-1}; the HFER sample had previously been pretreated in situ under nitrogen flow for 10 h at 500 °C. Regardless of the contact time τ (taken as the reverse of WHSV) and the TOS, the distribution of linear butenes was always close to that at thermodynamic equilibrium. Therefore, we calculated the conversion into the various products while considering *n*-butene isomers as the reactant.

Reaction products were analyzed on-line by FID gas chromatography with a 50-m fused silica Chrompack PLOT Al_2O_3/Na_2SO_4 capillary column. The analysis of the products was carried out for TOS long enough ($\geqslant$ 1 min) to attain

a constant value of the GC peak area and hence a constant value of the reactant pressure in the reactor.

The acidic properties of the HFER samples were characterized by ammonia and deuteroacetonitrile (CD_3CN) adsorption followed by IR spectroscopy on a Nicolet NEXUS IRTF spectrometer. The zeolite samples were pressed into thin wafers (18–24 mg, 2 cm^2) and then activated in situ. For fresh HFER, the activation procedure consisted of two steps: the first one under air flow (1 ml s^{-1}, atmospheric pressure) at 450 °C for a night, the second in vacuum (10^{-3} Pa) at 200 °C for 1 h. For the coked samples, only a treatment in vacuum at 175 °C for 1 h was applied. NH_3 was introduced in excess into the IR cell at 50 °C. The spectra were recorded after outgassing at the same temperature (10^{-3} Pa, 1 h) to eliminate the physisorbed molecules. Adsorption of CD_3CN was carried out at 175 °C with the introduction of successive doses up to a maximum height of the band at 2296 cm^{-1}, which corresponds to CD_3CN coordinated to Brønsted acid sites.

3. Results

3.1. Influence of time on stream on n-butene transformation

Regardless of the operating conditions (contact time τ, TOS), the main reaction products were isobutene, propene + pentenes in a molar ratio greater than 1 (from 2–2.5 at short TOS to 1.6 at 21.5–44 h), *n*-butane, C_6–C_8 alkenes, and ethylene. Low amounts of ethane, propane, isobutane, pentanes, and nondesorbed products (coke) could also be observed. Coke formation initially appeared to be very fast: 1.2 wt% C deposited on the zeolite in 5 min at $\tau = 0.077$ h (Fig. 1). However, this corresponds to a conversion of *n*-butenes of 0.14% only, that is, 250 times lower than the conversion into desorbed products. After a reaction time of 3 h, the deposition of coke becomes very slow: only 2.2 wt% C was deposited from 3 to 44 h (Fig. 1).

It is apparent that the deactivation of HFER that can be observed (Fig. 2) is due to the formation and trapping of "coke" within the zeolite micropores. Furthermore, the change in the yield in most of the products [propene +

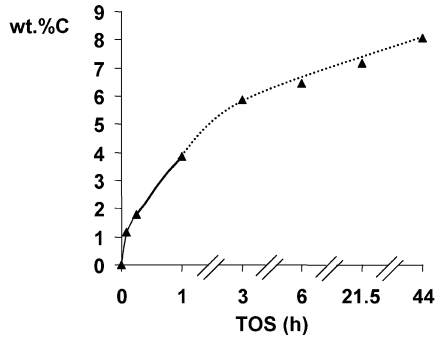

Fig. 1. Percentage of coke (wt% C) deposited on the HFER sample as a function of time-on-stream TOS (h).

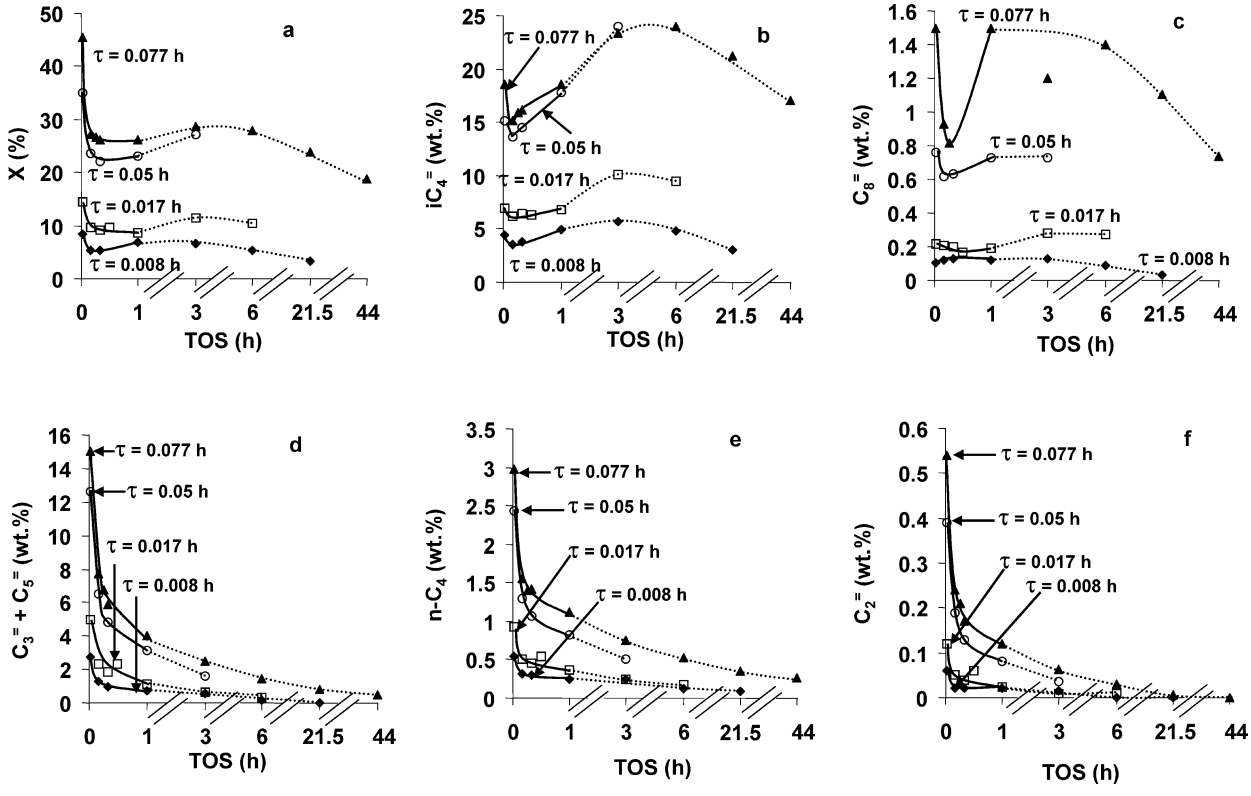

Fig. 2. Influence of time-on-stream TOS (h) on *n*-butene conversion (a) and on the yields in isobutene (b), octenes (c), propene + pentenes (d), *n*-butane (e), and ethylene (f).

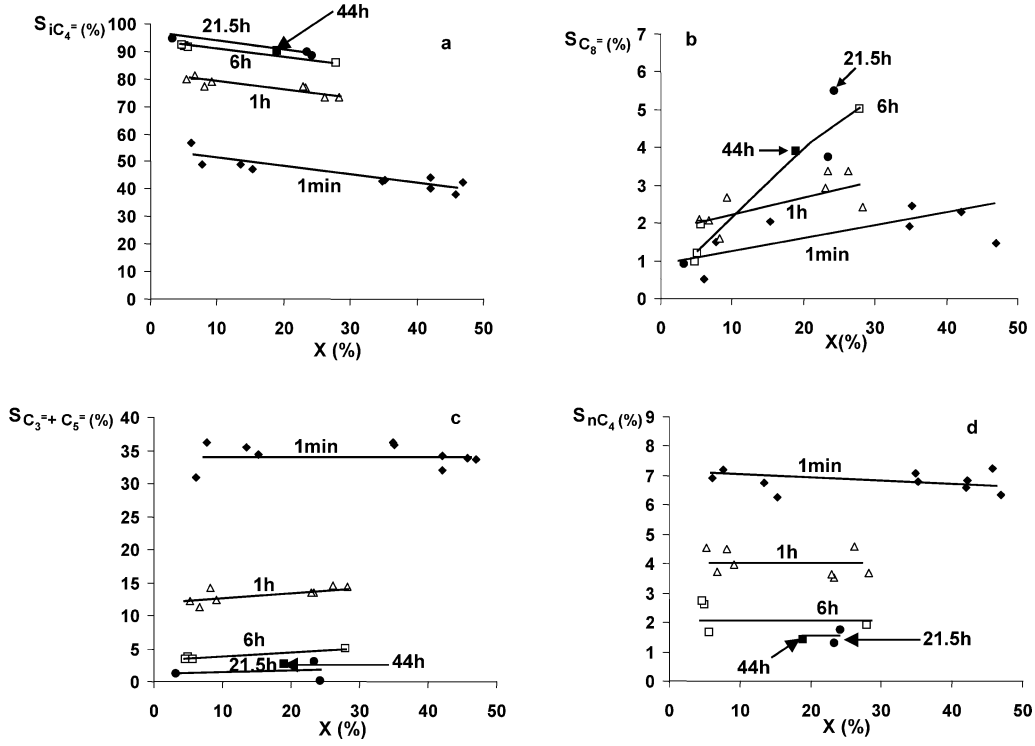

Fig. 3. Influence of *n*-butene conversion on the selectivities to isobutene (a), octenes (b), propene + pentenes (c), and *n*-butane (d) for time-on-stream values from 1 min to 44 h.

pentenes (Fig. 2d), *n*-butane (Fig. 2e), ethylene (Fig. 2f), hexenes, heptenes, etc.] is the one expected from the effect of TOS on coke formation (Fig. 1): a significant decrease in the first 10 min of reaction, then a more progressive decrease. The change with TOS of the yields in isobutene (Fig. 2b) and octenes (Fig. 2c) is more complex: an initial decrease followed by an increase then by a slow decrease; whatever the value of τ, the yields in isobutene and octenes are maximum for a TOS value between 3 and 6 h.

The difference between the shapes of the curves b, c and d, e, f in Fig. 2 has as a consequence a large change in selectivities with TOS (Fig. 3): a significant increase in the selectivity for isobutene at the expense of the selectivities for all of the other products except octenes (Fig. 3b). It should be remarked that *n*-butene conversion has practically no effect on the selectivity for isobutene (Fig. 3a), propene + pentenes (Fig. 3c), and *n*-butane (Fig. 3d), whereas the selectivity for octenes increases with *n*-butene conversion (Fig. 3b).

To determine the kinetic (primary, secondary) mode of formation of the various products and this for different TOS values, their yield was plotted as a function of contact time τ (Fig. 4):

- Isobutene (Fig. 4a) appears as a primary product with a secondary transformation at long contact time (high conversion). TOS has, at least up to 6 h, a limited effect on isobutene formation. Moreover, the secondary transformation is more pronounced at short than at long TOS, with consequently higher values of the yield in isobutene at long TOS for $\tau = 0.077$ h.
- Propene + pentenes (Fig. 4c) are also primary products with a secondary transformation; however, their production decreases significantly with increasing TOS.
- *n*-Butane (Fig. 4d) appears to be a primary product without any secondary transformation. The same thing can be observed for ethylene.
- Octenes (Fig. 4b) (but also heptenes and hexenes), which appear as primary products for TOS = 1 min, become secondary for TOS > 1 h. A secondary mode of octene formation can already be observed for TOS = 1 min (Fig. 4b).

All of this is confirmed by the plots of the yields as a function of *n*-butene conversion (not presented here).

For TOS values of 1 min, 1, 3, 6, and 21.5 h, the rates of formation of the primary products were estimated from the slopes of the initial tangents to the curves in Fig. 4. For TOS = 44 h, we estimated the activity for isobutene production by determining, on the curve in Fig. 4a for TOS equal to 6 h, the contact time (0.042 h) at which the yield in isobutene for TOS = 44 h would be obtained. The rate of isobutene formation at 44 h was assumed to be equal to the product of the rate at 6 h by the ratio of contact times, 0.042/0.077. As the conversion in the other products at $\tau = 0.077$ h is low, the rate of their production at 44 h was simply taken as the product of the rate at 6 h times the ratio of the yields at 44 h and at 6 h.

Table 1 shows that TOS has only a small effect on the rates of isobutene and octene production. These rates are 1.7

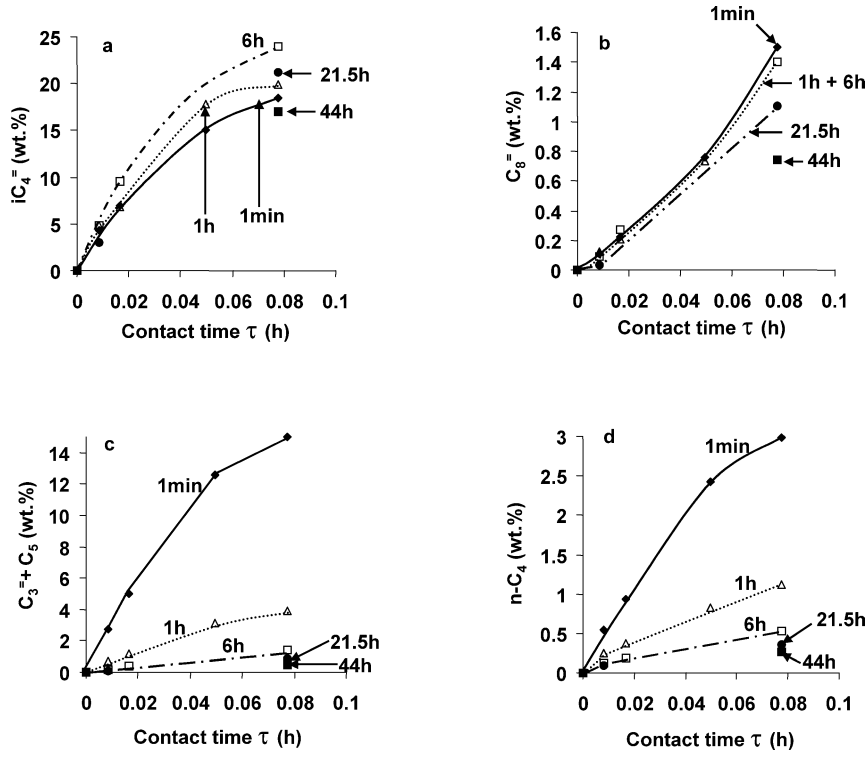

Fig. 4. Yields in isobutene (a), octenes (b), propene + pentenes (c), and *n*-butane (d) vs contact time τ (h) for time-on-stream values from 1 min to 44 h.

Table 1
Rates of formation of the primary products *r* (mmol of *n*-butene converted h^{-1} g^{-1}) at different time-on-stream (TOS) values (h). Residual rate (RR): ratio between the rates on HFER aged for 44 h and on fresh HFER (TOS = 1 min)

TOS (h)	*r* ($iC_4^=$)	*r* ($C_3^= + C_5^=$)	*r* (nC_4)	*r* ($C_8^=$)	*r* ($C_6^= + C_7^=$)	*r* ($C_2^=$)
1/60	94	58	12	2.5	7.5	1.3
1	105	15	4	2.5	1.2	0.4
3	122	8	2.5	2.5	0.3	0.2
6	104	4	1.5	2.5	0.2	0
21.5	65	1	0.8	2.3	0	0
44	55	0.5	0.6	1.7	0	0
RR	0.6	0.0085	0.05	0.7	0	0

Table 2
Yields (wt%) in the various products for a contact time τ of 0.077 h as a function of time-on-stream TOS

TOS (h)	$iC_4^=$	$C_3^= + C_5^=$	nC_4	$C_8^=$	$C_6^= + C_7^=$	$C_2^=$	Others
1/60	18.0	15.0	3.0	1.5	3.8	0.55	2.0
1	19.9	3.8	1.2	0.8	1.1	0.1	0.25
3	23.2	2.5	0.7	1.1	0.9	0.05	0.08
6	24.0	1.4	0.5	1.4	0.4	0.03	0.1
21.5	21.3	0.9	0.4	1.1	0.1	0	0
44	17.0	0.5	0.25	0.7	0	0	0
Residual yield	0.95	0.035	0.08	0.47	0	0	0

and 1.4 times lower at a reaction time of 44 h than initially (1 min). The effect of TOS is more pronounced for *n*-butane production (/20) and much more pronounced for the production of propene and pentenes (/120). Last, after 3 h of reaction, hexenes, heptenes, and ethylene are not observed at low conversion.

Another way to show the effect of TOS on the rates of product formation is to compare the yields at the same contact time. This was done in Table 2 for $\tau = 0.077$ h, which is the contact time for which the aged samples were characterized (Section 3.2). Under these conditions, the yields in isobutene for TOS = 1 min and 44 h are identical, the yield in octenes is divided by 2, and those in *n*-butane and propene + pentenes by 11 and 30, respectively. The trends are similar to those in rates (Table 1), but the differences between 1 min and 44 h are less pronounced.

3.2. Characterization of the aged HFER samples

As was previously shown [5], coke causes a dramatic decrease in the micropore volume accessible to nitrogen (Fig. 5a), and after 6 h of reaction at $\tau = 0.077$ h (6.5 wt% C), less than 5% of the micropore volume remains accessible. This pore blockage was confirmed by *n*-butane adsorption at room temperature on the HFER sample aged for 21.5 h (Fig. 5b). The micropore volume accessible to *n*-butane is very small: 0.003 cm^3 g^{-1}, equal to only 2% of the micropore volume of fresh HFER (0.154 cm^3 g^{-1}).

The OH region of the IR spectra of the fresh and of some aged samples is shown in Fig. 6. With the fresh sample, an intense and asymmetrical band is found at 3601 cm^{-1}; this band is ascribed to the stretch vibration of the bridging hydroxyl groups (SiOHAl). The band at 3747 cm^{-1} is assigned to the terminal silanol groups and the shoulder at 3639 cm^{-1}

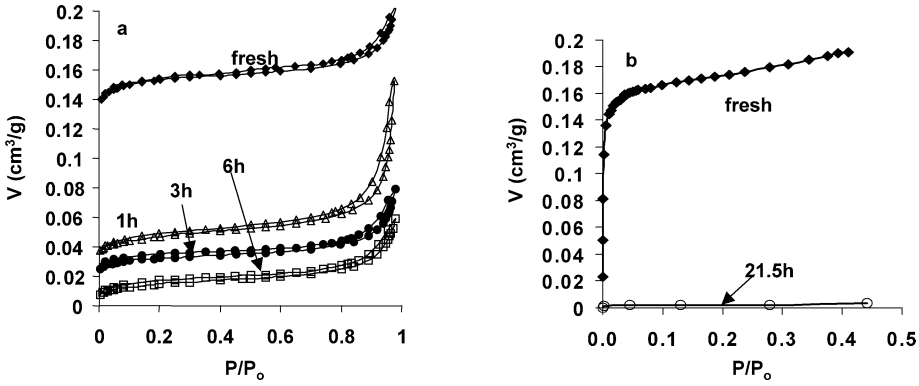

Fig. 5. (a) Isotherms of nitrogen adsorption at −197 °C over the fresh HFER sample and over samples aged for 1, 3 and 6 h (wt% C of 3.9, 5.9, and 6.5, respectively). (b) Isotherms of *n*-butane adsorption at 25 °C over the fresh HFER sample and over a sample aged for 21.5 h (wt% C of 7.2).

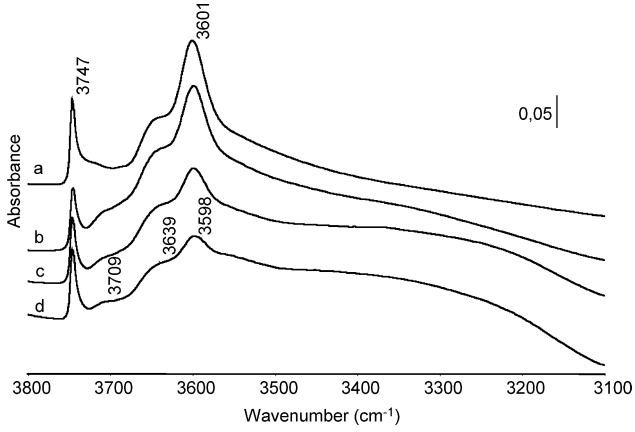

Fig. 6. Comparison of the hydroxyl region of the fresh HFER sample (a) and of samples aged for $\frac{1}{4}$ (b), 1 (c), and 6 h (d) (normalized for 10 mg of zeolite).

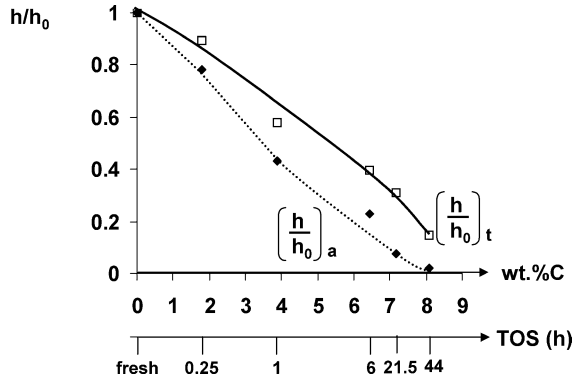

Fig. 7. Influence of coke content (wt% C) and of time-on-stream TOS (h) on the ratios $(h/h_0)_t$ and $(h/h_0)_a$ between the heights of the OH band at 3600 cm^{-1} of the aged and fresh HFER samples. t means total bridging hydroxyl band; a—accessible bridging hydroxyl band.

to hydroxylated extraframework Al species. Carbonaceous deposits (coke) cause a very pronounced decrease in the intensity of the bridging OH band, which shows that coke molecules interact with the corresponding protonic sites. This interaction is responsible for the formation of a broad band at approximately 3300 cm^{-1} (Fig. 6). This band probably corresponds to a shift of part of the bridging OH band at 3601 cm^{-1} to lower wavenumbers due to hydrogen bonding with coke molecules [31]. The effect of coke on the intensity of the bridging OH band was estimated from the normalized height of this band. Fig. 7 shows that the decrease in relative height $(h_t/h_0)_t$ is quasi-proportional to coke content. The bands that correspond to coke molecules are those previously described in Ref. [23]; the most intense band, which appears at 1523 cm^{-1}, can be ascribed to carbon–carbon bond vibration of noncondensed aromatics. The longer the TOS, and hence the greater the amount of coke, the higher the intensity of the corresponding bands.

Adsorption of NH_3 was carried out over the fresh and aged samples. Fig. 8 shows that after adsorption–desorption at 50 °C over the fresh HFER, there is a complete disappearance of the bridging OH band, a decrease in the shoulder at 3564 cm^{-1} (extraframework Al species), and practically no effect on the silanol band. A similar effect of NH_3 can be observed with the aged samples, except that part of the residual bridging OH groups do not interact with NH_3. This indicates that the access of NH_3 to these hydroxyl groups (and of course the access of the bulkiest reactant molecules) is blocked by carbonaceous deposits. A comparison of the relative heights of the bands for the total residual bridging OH groups, $(h/h_0)_t$, and for the accessible groups (interacting with NH_3), $(h/h_0)_a$, shows that the higher the coke content, the more significant the blockage (Fig. 7). Thus the percentage of residual bridging OH groups found to be inaccessible was 25% after 1 h of reaction (3.9 wt% C) and 75% and 85% after 21.5 h (7.2 wt% C) and 44 h (8.1 wt% C), respectively.

Another estimation of the accessible OH groups was made from the surface of the hydroxyl bands in Fig. 9 from 3670 and 3465 cm^{-1}. We calculated three series of values: one by considering all of the OH bands in this region, that is, those corresponding to bridging OH groups and to hydroxylated extraframework Al species (band at 3639 cm^{-1}); another by considering only the bridging OH groups after a deconvolution treatment similar to the one applied by Domokos et al. [32]; and the last by considering only the bridging OH groups in the 10-MR channels. Indeed, ac-

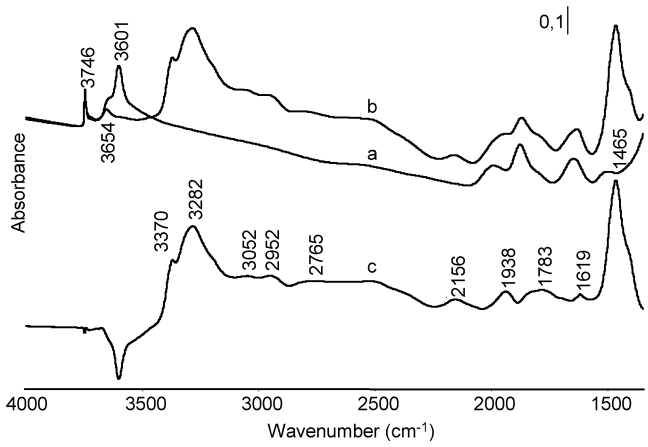

Fig. 8. Characterization of the fresh HFER sample by NH_3 adsorption. (a,b): spectra of the fresh sample after activation and after NH_3 adsorption–desorption at 50 °C, (c) difference spectrum (b − a) (normalized for 10 mg of sample).

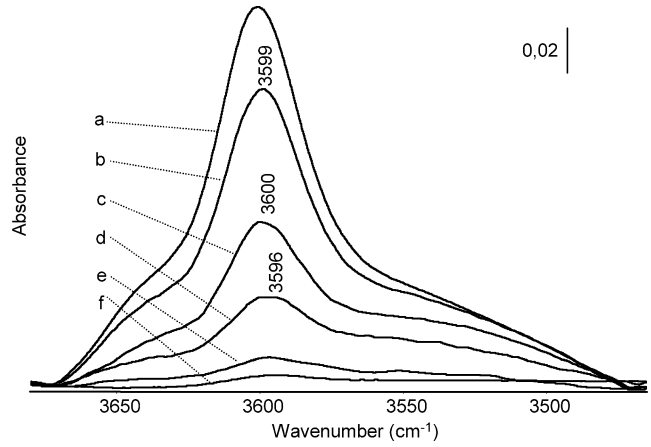

Fig. 9. Influence of aging on the hydroxyl bands interacting with NH_3 (normalized for 10 mg of sample). Fresh HFER (a), sample aged for $\frac{1}{4}$ (b), 1 (c), 6 (d), 21.5 (e), and 44 h (f).

cording to several authors [18,32,33], these latter sites could be the only active sites for *n*-butene transformation into isobutene. Table 3 shows that the effect of coke content on the relative values of the surface of the hydroxyl bands does not depend very much on the bands that are considered.

The main bands of chemisorbed NH_3 can be observed in Fig. 8: at 3370 and 3283 cm^{-1}, which correspond, respectively, to asymmetrical and symmetrical stretching vibration and at 1465 cm^{-1}. This last band (δ_{as} NH_4^+) can be used for the estimation of the Brønsted acidity. However, because of the appearance for TOS > 1 h of coke bands in the same position, this estimation can be carried out only for the fresh sample and for the samples aged for $\frac{1}{4}$ h and 1 h. Whereas the value found for the sample aged for $\frac{1}{4}$ h is in agreement with the decrease in the OH band intensity, that found after 1 h of reaction is much higher than expected (Table 3). This suggests that even for this short reaction time, there is some overlap of the NH_4^+ and coke bands. However, a partial desorption of coke molecules from the protonic sites by the small and very basic NH_3 molecules is also possible [34].

The quantification of the Brønsted acidity by adsorption of deuteroacetonitrile (CD_3CN) does not present this limitation [20]: there are no coke bands in the ν(CN) stretching region (2600–2100 cm^{-1}). This is why we have used this method to determine the change in acidity with carbonaceous deposits. The experiments were carried out with fresh HFER and with the samples aged for 6 and 44 h. The spectra obtained with fresh HFER before and after CD_3CN adsorption and the difference spectrum are presented in Fig. 10. The spectrum after CD_3CN adsorption shows well-established contours at ∼ 2800 and ∼ 2420 cm^{-1}, respectively, which result from a large red shift of the bridged hydroxyl band at 3600 cm^{-1} due to hydrogen bonding to the nitrogen atoms. The peaks at 2296 and 2332 cm^{-1} are assigned to the stretching vibration of ν(CN) coordinated with Brønsted and Lewis sites, respectively. Furthermore, CD_3CN adsorption causes the total disappearance of the bridging OH band at 3601 cm^{-1} and of the band

Table 3
Influence of time-on-stream (TOS) and coke content (C) on the intensity of the OH, NH_4^+ and CD_3CN–H^+ bands and average values of the total and 10-MR protonic acidity[a]

TOS	*C*	OH band			NH_4^+ band	CD_3CN on H^+	Protonic acidity (μmol g^{-1})	
(h)	(wt%)	$(S/S_0)_t$	$(S/S_0)_b$	$(S/S_0)_{10\text{-MR}}$	h/h_0	S/S_0	Total	10-MR
(1)	(2)	(3)	(4)	(5)	(6)	(7)	(8)	(9)
0	0	1	1	1	1	1	896	360
1/4	1.8	0.81	0.85	0.80	0.84		760	290
1	3.9	0.51	0.51	0.34	0.72[b]		460	120
6	6.5	0.28	0.26	0.20		0.14	150	70
		(0.14[c])	(0.11[c])	(0.07[c])				
21.5	7.2	0.075	0.06	0.055			55	40
44	8.1	0.01	0.015	0.035		0.055	35	13
		(0.05[c])	(0.04[c])	(0.03[c])				

[a] $(S/S_0)_t$, $(S/S_0)_b$, $(S/S_0)_{10\text{-MR}}$: values of the relative surface of the "acidic" OH band (3670–3465 cm^{-1}), of the bridging and 10-MR OH bands, respectively.

[b] Not valid (see in text).

[c] Drawn from CD_3CN adsorption experiments.

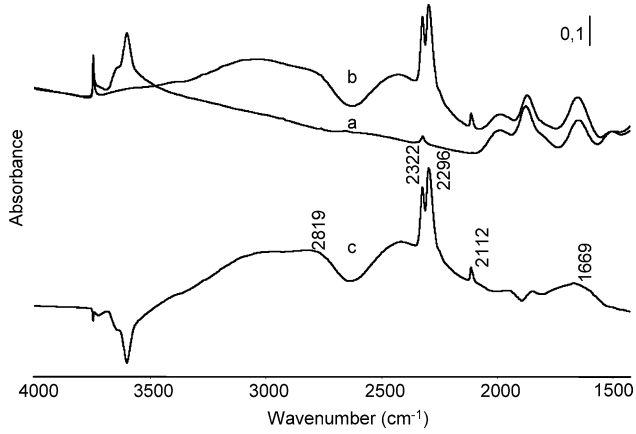

Fig. 10. IR spectra of fresh HFER after activation (a) and after deuteroacetonitrile adsorption (b) and the difference spectrum (b − a) (normalized for 10 mg of sample).

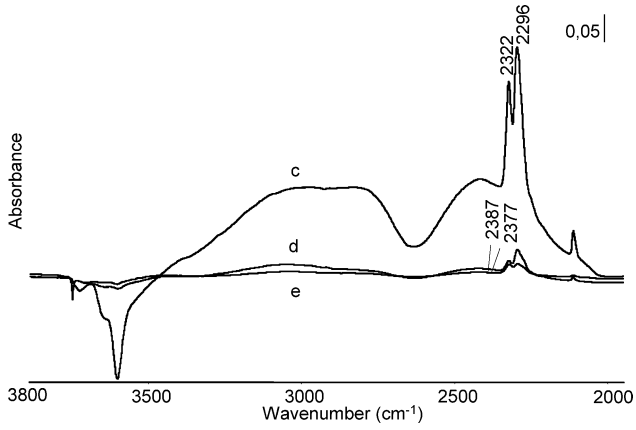

Fig. 11. IR difference spectra of deuteroacetonitrile adsorbed on fresh HFER (c) and on the samples aged for 6 (d) and 44 h (e) (normalized for 10 mg of sample).

at 3639 cm^{-1} ascribed to hydroxylated extraframework Al species with Lewis acidity. A small decrease in the intensity of the silanol band at 3747 cm^{-1} can also be observed (Fig. 10).

With the samples aged for 6 and especially for 44 h, CD_3CN adsorption leads to only a partial disappearance of the bands at 3601 and 3639 cm^{-1} (Fig. 11). This observation confirms those made for NH_3 adsorption indicating that part of the Brønsted and Lewis sites of coked HFER samples are no more accessible by adsorbate and hence by the reactant molecules. Furthermore, as could be expected, the intensities of the bands at 2296 and 2332 cm^{-1} decrease significantly with coke content. The relative values of the Brønsted acidity drawn from CD_3CN adsorption are different from the relative values of the accessible bridging OH groups: lower after 6 h and higher after 44 h (Table 3).

The total concentration of protonic sites (or of bridging OH groups) interacting with base molecules was calculated for the aged HFER samples from the concentration of these sites in the fresh sample estimated by NH_3 adsorption (896 μmol g^{-1}) and from the relative values of the Brønsted acidity reported in columns 4, 6, and 7 of Table 3. The average values of this concentration are reported in column 8 of Table 3. The concentration of the 10-MR protonic sites interacting with base molecules was also estimated. Deconvolution of the bridging OH band of the fresh HFER shows that approximately 40% of the bridging OH groups are located in the 10-MR channels, which is quite similar to the value found by Domokos et al. [32] for a HFER8 sample. Therefore, the concentration of protonic sites in the 10-MR channels of fresh HFER was taken as equal to 40% of the total concentration (column 9 in Table 3). We calculated the corresponding values for the aged samples by multiplying the concentration in the fresh sample by the relative values reported in column 5 of Table 3. All of these estimations of site concentrations can be considered only semiquantitative. Indeed, we have assumed that the extinction coefficients of the bridging OH groups and of NH_3 or CD_3CN bonded to protonic acid sites were not different from one sample to another, whereas despite the quasi-identical thickness of the wafers used for FTIR experiments, there could be differences between the extinction coefficients of fresh and aged HFER samples. Moreover, for the very aged HFER sample, the estimation of the surface of the IR bands is not very accurate.

Adsorption of acetonitrile over zeolites in the presence of alkenes was shown to result in the appearance of bands at 2387 or/and 2376 cm^{-1}, which were ascribed respectively to secondary and tertiary carbenium ions complexed to CD_3CN [35,36]. These bands and bands in the same region corresponding to a nitrilium complex involving a primary benzylic carbocation cannot be observed in Fig. 11.

3.3. Activities of the accessible protonic sites of fresh and aged HFER samples

The activities of the protonic sites for the formation of the main primary products (their TOFs) were calculated from the rates in Table 1 and from the concentrations of accessible protonic sites in Table 3 (column 8: total concentration; column 9: concentration of the 10-MR sites). The TOF values for isobutene production calculated from the total concentration of sites are not very different here (Table 4) from those reported in Ref. [20]: quasi-identical values are obtained at 6.5 wt% C, whereas at a higher coke content, lower values are found (Ref. [20]).

Table 4 shows that with both estimations, there is a significant increase with TOS in the TOF values for isobutene production: × ∼ 15 from 1 min to 44 h. The same can be observed for octene production, whereas the TOF values for propene + pentenes and *n*-butane production do not depend very much on TOS. The limit values indicated on the last line in Table 4 show that despite the relatively large uncertainty in the estimation of the acid site concentration, the positive effect of TOS on the TOF in isobutene and octene production cannot be questioned.

Table 4
Average turnover frequency (TOF) values calculated from the total and 10-MR into concentrations of protonic acid sites

TOS	C	Average TOF values (h^{-1})			
(h)	(wt%)	$iC_4^=$	$C_3^= + C_5^=$	nC_4	$C_8^=$
1/60	0	105 (260)	65 (160)	13 (33)	3 (7)
1	3.9	230 (875)	33 (125)	9 (33)	5.5 (20)
6	6.5	690 (1500)	27 (60)	10 (20)	17 (35)
21.5	7.2	1200 (1630)	18 (25)	15 (20)	42 (60)
44	8.1	1570 (4200)	14 (40)	17 (45)	49 (130)
$TOF_{44}/TOF_{1/60}$		15 (16)	0.21 (0.25)	1.3 (1.4)	16 (19)
[a]		10–40	0.15–0.6	1–3.5	10–40

[a] Values obtained by considering the extreme values of the concentration of residual protonic sites.

4. Discussion

4.1. Effect of time on stream on the isobutene yield: toward a monomolecular or a pseudomonomolecular pathway?

The simultaneous direct formation of propene, pentenes, and isobutene that was observed on fresh HFER shows the predominance of bimolecular reactions. Not only are propene, pentenes, and (at least) a large part of isobutene formed through a bimolecular pathway (Scheme 1), but so are most of the other products: *n*-butane, C_6–C_8 alkenes, and carbonaceous compounds trapped in the micropores (coke). Moreover, a fast alkylation of pentenes by butenes followed by cracking steps (Scheme 3) is most likely responsible for a propene/pentene molar ratio higher than 1.

The selectivity for isobutene increases significantly with TOS, from approximately 50% over the fresh HFER (TOS = 1 min) to more than 90% after 20 h of reaction (Fig. 3a). This increase occurs essentially at the expense of propene + pentenes and hence could be explained by the change from a predominant bimolecular mechanism over fresh HFER to a predominant monomolecular mechanism over the aged HFER samples.

However, as was previously mentioned [37], this simple explanation cannot account for the increase in isobutene yield observed after the initial decrease (Fig. 2b). Such an increase is generally found for experiments carried out at high conversion, that is, when thermodynamic equilibrium between *n*-butenes and isobutene is practically established, which is the case in many studies [10,12,15,16,18,25,38–40]. Under these conditions, this increase can be related to the suppression of secondary nonselective dimerization–isomerization–cracking transformation of isobutene: coking causes a decrease in *n*-butene conversion and less isobutene is converted into by-products, with an apparent increase in the formation of this desired product [10,41]. This explanation should not be valid at a low conversion like that in this work (Fig. 2). Indeed, this would demand that isobutene transforms much more rapidly than *n*-butenes into propene and pentenes, whereas the reverse was found [5]. Moreover, a high rate of isobutene transformation would result in an apparent secondary formation of propene and pentenes, which is not observed; the yields in propene and pentenes are proportional to contact time (Fig. 4c) and to *n*-butene conversion up to relatively high conversion values. A significant decrease in the selectivity for isobutene with increasing *n*-butene conversion should also be observed, although only a limited decrease is found (Fig. 3a). Therefore, the increase in isobutene yield shown in Fig. 2b actually corresponds to an increase in the rate of *n*-butene transformation into isobutene and hence can only be explained by the development of a selective isomerization pathway that does not exist on the fresh HFER sample.

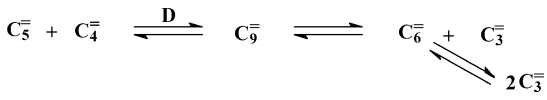

Scheme 3.

This new isomerization process was proposed [37] to be an autocatalytic pathway (Scheme 4); *n*-butene isomerization would occur on *tert*-butyl carbenium ions, that is, on isobutene adsorbed on protonic sites.

Indeed, this isomerization of *n*-butenes over *tert*-butyl carbenium ions (Scheme 4) involves more facile steps than the classical bimolecular process. In particular, step 1 of Scheme 4, which involves one tertiary and one secondary carbenium ion, is much faster than the first step of the bimolecular mechanism, the alkylation of *n*-butene by 2-butyl carbenium ion, which involves two secondary carbenium ions [5].

This pathway should be very selective to isobutene. Indeed, the formation of propene and pentenes (Scheme 5) involves more steps than the formation of isobutene. The last

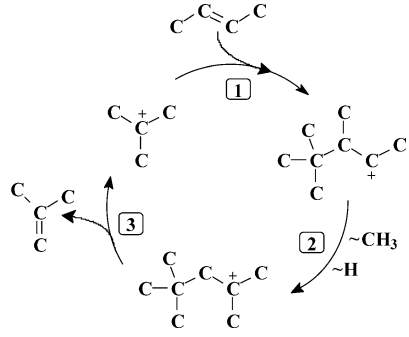

Scheme 4. Autocatalytic mechanism of *n*-butene isomerization. *tert*-Butyl carbenium ions are the active species.

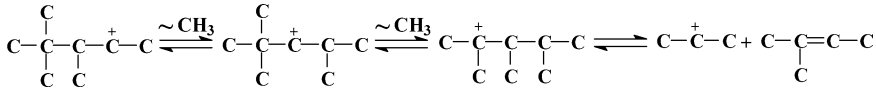

Scheme 5.

of these occurs with the formation of a secondary carbenium ion (Scheme 5) and is much slower than step 3 of the autocatalytic process (Scheme 4), which involves two tertiary carbenium ions.

This autocatalytic pathway is pseudomonomolecular, that is, only one molecule of *n*-butene is involved per catalytic cycle. Therefore, the number of ^{13}C in isobutene molecules resulting from the transformation of ^{13}C-labeled *n*-butene through this mechanism will be equal to the number of ^{13}C in the reactant, as is the case with a classical monomolecular mechanism. This means that the large differences that were found in the composition of isobutene resulting from the transformation of *n*-butene containing one ^{13}C atom over fresh and aged samples can also be explained by the progressive substitution with TOS of a purely bimolecular mechanism by this pseudomonomolecular mechanism. An additional argument in favor of this proposal is that the ^{13}C distribution found with fresh HFER samples is the one expected from a bimolecular pathway [16,25] and not from the coexistence of mono- and bimolecular pathways.

However, the one condition for the development of this autocatalytic pathway is a long residence time of isobutene within the HFER micropores. This long residence time seems most likely when the pore structure of the FER zeolite and the size of the isobutene molecule are considered. Indeed, the kinetic diameter of isobutene (≈ 5.0 Å) is slightly larger than the pore entrance of the 8-MR (eight O atoms in the aperture) channels (3.5 × 4.8 Å), making diffusion of this molecule through these channels improbable. This is confirmed by the high activation barrier (160 kJ mol^{-1}) calculated for this diffusion [42,43]. The pore entrance of the long 10-MR channels is larger (4.2 × 5.4 Å), and the diffusion of isobutene molecules through these channels is quite possible. However, the activation barrier is relatively high, and limits in the desorption of isobutene molecules from the 10-MR channels are most likely [42,44]. In contrast, no limitation in the diffusion of *n*-butenes can be expected. Indeed, there is more than one order of magnitude difference between the self-diffusion coefficients of *n*-butenes and isobutene estimated at 350 °C (14 times greater for *trans*-2-butene than for isobutene) [42]. Therefore, it can be concluded that the production of isobutene (and of the other branched products) can occur in the 10-MR channels, but not in the 8-MR channels; because of diffusion limitations, their residence time there is relatively long, making an autocatalytic pathway most likely.

A definitive argument against the participation of a monomolecular pathway in isobutene formation can be made from a comparison between the rates of isobutene production over the fresh and very aged HFER samples (Table 1) or between the activities of their protonic sites (TOF) accessible to base molecules (Table 4). Indeed, although the TOF value for isobutene production obtained over aged HFER samples (predominant monomolecular mechanism) should be much lower, or at least lower, than that obtained over the fresh sample (predominant bimolecular mechanism), it is the opposite which is observed. Thus, with the HFER sample aged for 44 h, the TOF value for isobutene production is 15 times higher than that obtained with the fresh HFER sample (Table 4). Practically the same difference in TOF can be observed when the protonic sites of the 10-MR channels (Table 4), which would be the only inner sites able to catalyze *n*-butene isomerization, are considered.

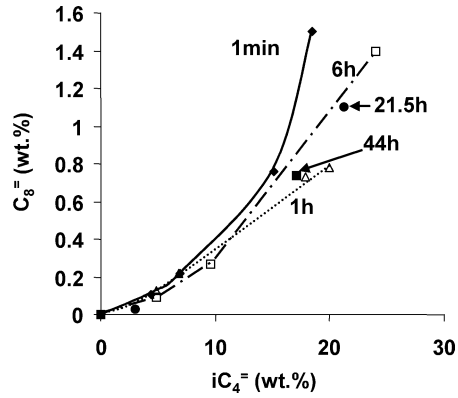

Fig. 12. Yield in octenes vs the yield in isobutene for time-on-stream values between 1 min and 44 h.

In contrast, TOS has a pronounced effect on the rates of propene + pentenes and *n*-butane production, which could be expected from the decrease in the concentration of accessible protonic sites, while the TOF values are practically constant (Table 4). This is surprising for *n*-butane formation, which occurs from hydride transfer from carbonaceous deposits to *n*-butene. Indeed, a positive effect of the acid site density on the TOF for this bimolecular reaction has been found over cracking FAU catalysts [45]. The too high value observed here with the very aged HFER samples could be related to the possibility that *n*-butene (and *n*-butane) molecules have to diffuse through the 8-MR channels.

Furthermore, the change with TOS of the rate and TOF value for octene production is similar to that observed for isobutene (Tables 1 and 4). This observation suggests that a large part of octenes result from a fast (but thermodynamically limited) secondary transformation of isobutene: dimerization or *n*-butene–isobutene codimerization. The form of the plot of the octene yield versus the isobutene yield (Fig. 12) is in good agreement with this proposal: octenes appear only for yields in isobutene greater than 5%. Essentially trimethylpentenes result from isobutene transformation; these molecules, which are too bulky to desorb from the inner micropores [24], are most likely formed at the pore mouth.

Although the autocatalytic pathway provides a simple explanation for the change in the rate of isobutene production with TOS, other pseudomonomolecular mechanisms have been proposed [4,23,46] in particular to explain the catalytic behavior of HFER samples that have been aged for a long time. As the access of nitrogen to most of their micropores was blocked and most of the protonic sites poisoned or made inaccessible by carbonaceous compounds (coke), it was as-

sumed that *n*-butene isomerization was no longer catalyzed by "naked" protonic sites but by carbonaceous compounds (coke) chemisorbed on protonic sites near the micropore mouth [23]. Benzylic cations, the stability of which is similar to that of tertiary carbenium ions, formed from methylaromatics trapped within the HFER micropores at the vicinity of their mouth, were proposed as active species [23]. Alkyl-substituted cyclopentenyl cations detected by ^{13}C CP/MAS NMR during transformation of ^{13}C *n*-butene were also advanced as active species [46]. All of the steps involved in the isomerization mechanism over these proposed species were shown to be very facile and to lead selectively to isobutene as the autocatalytic pathway does.

Pore blockage and deactivation of the protonic sites by coke were confirmed in this work. Thus, less than 5% of the micropore volume was still accessible to nitrogen after only 6 h of reaction time (6.5 wt% C). Moreover, only 2% of the micropore volume was accessible to *n*-butane at room temperature after 21.5 h of reaction time (7.2 wt% C). This latter observation shows that the low values of the accessible micropore volumes obtained by nitrogen adsorption at −197 °C are not due to the lack of mobility and flexibility of coke molecules at this low temperature, which therefore would more easily block access to the micropores. Furthermore, most of the protonic sites were shown to be poisoned or made inaccessible by carbonaceous compounds. However, as emphasized by van Donk et al. [18,20], vacant Brønsted sites are still present, even after very long reaction times. Hence over the aged HFER samples, the selective skeletal isomerization of *n*-butene could occur on "naked" protonic sites. In agreement with this proposal, no bands corresponding to deuteroacetonitrile bound to carbocations [35,36] can be observed in the IR spectra of aged HFER samples after CD_3CN adsorption. However, this does not constitute a definitive argument against the participation of carbonaceous species in isobutene formation. Indeed, the IR experiments are carried out under conditions (in vacuum) different from those of the catalytic experiments in particular in the absence of *n*-butene molecules, whereas these molecules are most likely involved in the formation of benzylic cations i.e. hydride transfer from methylaromatic to secondary butylcarbenium ions.

4.2. Pore system and acidity of HFER zeolites and selectivity for isobutene

Whereas the increase with TOS in the selectivity and TOF values for isobutene production can be explained by the progressive replacement of the bimolecular pathway with an autocatalytic pathway, an important question remains to be answered: How can the pore system or/and the acidity of HFER favor this selective autocatalytic pathway? To answer this question, we propose below a simplified model of the catalytic transformation of *n*-butene within the HFER micropores. This model is based on the following assumptions:

- Most of the *n*-butene transformations occur within the large 10-MR channels only.
- In these channels, *n*-butene isomerization occurs only through the bimolecular and the autocatalytic mechanisms.
- In the 10-MR channels, reactant and product molecules can essentially diffuse in single file [21]. Counter-diffusion is limited, and molecules entering one channel have to diffuse along this channel without any possibility of desorption before the exit. Therefore, the 10-MR channels can be considered noninterconnected nanoreactors operating in parallel.

The particular catalytic properties of this system of nanoreactors have previously been demonstrated in *m*-xylene isomerization over acidic mesoporous MCM-41 catalysts [47,48]. Over these catalysts, *m*-xylene isomerization does not occur through the classical monomolecular mechanism but through a bimolecular pathway. This bimolecular pathway involves *m*-xylene disproportionation into toluene and trimethylbenzenes, followed by a series of rapid steps of transalkylation between *m*-xylene and trimethylbenzenes with the preferential formation of *o*-xylene. This particular behavior was proposed to be due to the noninterconnected long channels of MCM-41 catalysts: *m*-xylene molecules have to diffuse along the channels without any possibility of desorption before the exit and hence undergo various successive reaction steps. This new mode of shape selectivity related to the length of noninterconnected channels was called Tunnel Shape Selectivity [48].

Let us examine the consequences that can be expected from this simple model for the rate and selectivity of *n*-butene transformation. In each of the independent 10-MR channels, the larger the number of protonic sites along the channels (and the higher the *n*-butene partial pressure), the greater the number of successive reactions undergone by *n*-butene molecules. Therefore, the products desorbing from each of the 10-MR channels could be completely different (Fig. 13):

(i) In the channels with few protonic sites, the *n*-butene molecules could undergo only a limited number of successive reactions (Fig. 13a), and the conversion of *n*-butene will be low. After a nonselective bimolecular process over protonic sites near the entrance of the 10-MR channels, *n*-butene molecules will undergo a selective isomerization into isobutene on tertiary carbenium ions resulting from isobutene adsorption on other protonic sites (autocatalytic process). At a low conversion level, the role played by the autocatalytic process will be predominant and isobutene will be selectively formed.

(ii) In the channels with a large concentration of protonic sites, *n*-butene molecules will undergo a significant number of successive reactions (Fig. 13b), with the consequent formation of a thermodynamically equili-

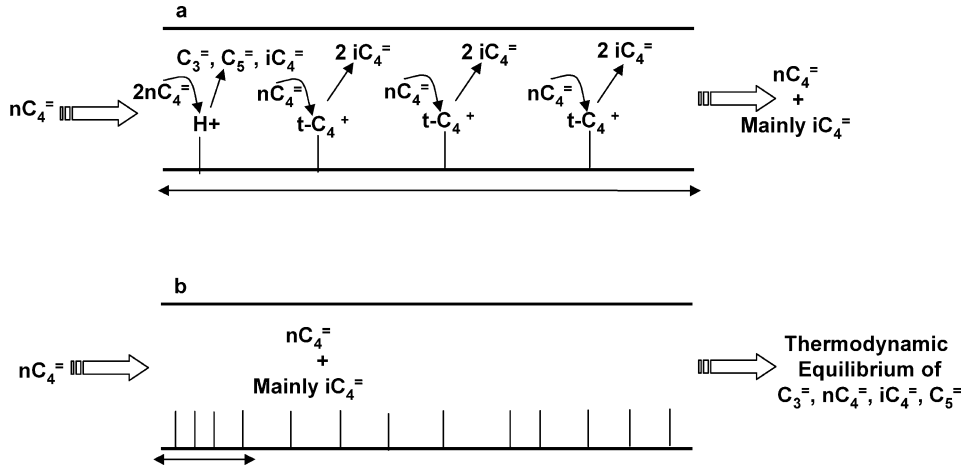

Fig. 13. Influence of the concentrations of protonic sites in the 10-MR channels of HFER on the products of *n*-butene transformation. (a) Channel with few protonic sites, low conversion of *n*-butenes, mainly isomerization through an autocatalytic pathway; (b) channel with a large number of protonic sites, high conversion of *n*-butenes with consequently production of an equilibrium mixture of $C_3^=$, $nC_4^=$, $iC_4^=$ and $iC_5^=$. In the first part of the channel (⟷), *n*-butene transformation occurs like in (a). | Corresponds to an active site.

brated mixture of all of the products: butenes, propene, pentenes, etc. An estimation of the composition of this mixture was made by considering the following formal equation:

$$\text{Propene} + \text{Pentenes (iso} + n) = \text{Butenes (iso} + n) \quad (6)$$

in which pentenes and butenes are supposed to be in their thermodynamic equilibrium *n*–iso mixture. A thermodynamic equilibrium constant of 0.9 was found for reaction (6), which leads to a mixture comprising 52.5% propene + pentenes and 47.5% butenes (25.2 and 22.3% of isobutene and *n*-butenes, respectively). The propene–pentenes–isobutene mixture would thus contain 32.5 wt% isobutene for 67.5 wt% propene + pentenes. Another important remark is that in these channels, the apparent activity of the protonic sites (TOF) is low, since most of them are used only for secondary transformations.

The product mixture at the exit of the zeolite cristallites is the sum of all the mixtures exiting from the parallel channels and hence has a composition intermediate between those obtained in cases (i) and (ii). Over a fresh zeolite with a high concentration of protonic sites (e.g., HFER with a low Si/Al ratio), at a high partial pressure of *n*-butene, *n*-butene molecules entering the channels would be transformed into a quasi-thermodynamically equilibrated mixture of butenes, propene, and pentenes. In contrast, in each of the channels of zeolites with a low concentration of protonic sites (e.g., HFER with a high Si/Al ratio), especially when they are exposed to a low partial pressure of *n*-butene, *n*-butene will be transformed selectively into isobutene through the autocatalytic process. This is exactly what is found. On the one hand, a high selectivity for isobutene can be observed for HFER samples with a high Si/Al ratio [49,50] and for very low partial pressures of reactant [10,44]. On the other hand, a very low selectivity, close to that expected in case (ii), was found for *n*-butene transformation over a HFER sample with a Si/Al ratio of 6 used under the operating conditions of this work [51]. On fresh HFER10, the composition is intermediate between cases (i) and (ii): there is formation of approximately 40 wt% propene and pentenes for 60 wt% isobutene.

The change in activity and selectivity for isobutene with TOS can also be explained through this simple model. The formation (and trapping) of coke molecules essentially at the intersection of the 8- and 10-MR channels [24] blocks the diffusion of molecules in the corresponding 10-MR channels. Various successive reactions steps are involved in the formation of coke molecules, which, consequently, occurs preferentially in the channels containing many protonic sites. Coke formation is also faster in these channels because of the nature of the octene intermediates and of the formation of nonenes (Scheme 3). Indeed, one essential step of coke formation is the cyclization of long-chain olefins into methylcyclopentadiene species [52]. In the channels containing few protonic sites, isomerization is essentially autocatalytic, with trimethylpentenes as intermediates. A direct cyclization of trimethylpentenes would require a primary carbenium ion as an intermediate (reaction (7)) and hence should occur very slowly; for example,

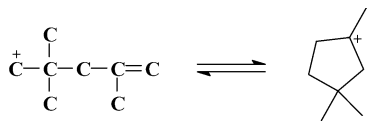

(7)

On the other hand, in the channels containing many protonic sites, octene intermediates are most likely in their thermodynamic equilibrium mixture, and, moreover, nonenes are formed (Scheme 3). Cyclization of various octenes (*n*-octenes, methylheptenes, and dimethylhexenes) and of nonenes, which involves only stable carbenium ion interme-

diates, for example,

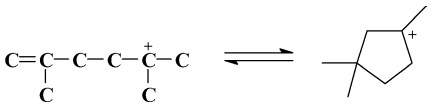

(8)

can easily occur, and hence coke formation is very fast.

Therefore on aged samples, *n*-butene transformation would occur in the nonblocked channels, which are those in which the concentration of protonic sites is very low, and hence for which the selectivity for isobutene and the apparent activity of the protonic sites (TOF) are high. However, linear molecules engaged in the 10-MR channels that are blocked by carbonaceous compounds could diffuse to the neighboring 10-MR channels through the 8-MR channels. This new diffusion path could contain fewer protonic sites than complete 10-MR channels and therefore has a higher selectivity for isobutene (essentially through the autocatalytic pathway) and a higher value of TOF for the residual protonic sites.

The increase in isobutene yield that is observed at relatively short TOS over low Si/Al HFER samples ($\leqslant 12$) can also be explained from this simple model of parallel independent nanoreactors. Indeed, along the new diffusion path, which contains fewer acidic sites than the 10-MR channels of fresh HFER, there are fewer secondary transformations of isobutene into by-products, with an apparent increase in the formation of this desired product. This increase occurs even at low conversion because the products result from the desorption of mixtures with different degrees of conversion from 10-MR channels with different concentrations of protonic sites. This increase cannot be observed over high Si/Al HFER samples, because in their 10-MR channels secondary transformations of isobutene are very limited.

5. Conclusion

The effect of TOS on the activity and selectivity of a HFER zeolite with a Si/Al ratio of 10 and on the concentration of residual accessible protonic sites was determined. The selectivity of the fresh zeolite was typical of a bimolecular *n*-butene dimerization–isomerization–cracking pathway with the simultaneous production of isobutene and propene + pentenes. Carbonaceous compounds trapped within the micropores (coke) cause a rapid decrease in the production of propene and pentenes, whereas the production of isobutene passes through a maximum. Therefore, on the aged samples, the selectivity of *n*-butene transformation into isobutene is very high (> 90% after 44 h of reaction time). Moreover, the turnover frequency for isobutene production of the accessible protonic sites is much higher (15 times after 44 h) than it is over fresh HFER; this allows us to reject the proposal generally advanced for a monomolecular isomerization mechanism over aged HFER samples.

A new proposal is advanced to explain the change with TOS in the activity and selectivity of HFER samples: the 10-MR channels of HFER can be considered as nanoreactors operating independently with a different product composition at their exits. From the channels containing many protonic sites, there is desorption of the thermodynamic equilibrium propene–pentene–butene mixture, whereas in those containing few protonic sites, isobutene is selectively formed through an autocatalytic mechanism. Coke formation is very fast in the first type of channels, leading to a rapid blockage of their access, and very slow in the second type of channels. Therefore, deactivation causes a significant increase in selectivity for isobutene. This simple proposal also provides an explanation of the increase in selectivity for isobutene of fresh HFER samples with their Si/Al ratio or with a decreasing partial pressure of *n*-butene.

References

[1] P. Grandvallet, K.P. de Jong, H.H. Mooiweer, A.G.T.G. Kortbeek, B. Kraushaar-Czarnetzki, European Patent 501577 (1992).
[2] J. Haggin, C & EN, 25 October 1993, 30.
[3] H.H. Mooiweer, K.P. de Jong, B. Kraushaar-Czarnetzki, W.H.J. Stork, B.C.H. Krutzen, in: J. Weitkamp, H.G. Karge, H. Pfeifer, W. Hölderich (Eds.), Zeolites and Related Microporous Materials: State of the Art 1994, in: Stud. Surf. Sci. Catal., vol. 84C, Elsevier, Amsterdam, 1994, p. 2327.
[4] M. Guisnet, P. Andy, N.S. Gnep, C. Travers, E. Benazzi, J. Chem. Soc., Chem. Commun. (1995) 1685.
[5] M. Guisnet, P. Andy, N.S. Gnep, E. Benazzi, C. Travers, J. Catal. 158 (1996) 551.
[6] M. Bjorgen, K.-P. Lillerud, U. Olsbye, S. Bordiga, A. Zecchina, J. Phys. Chem. B 108 (2004) 7862.
[7] M. Guisnet, PhD thesis, 1970, Poitiers.
[8] H. Pines, W.O. Haag, J. Am. Chem. Soc. 82 (1960) 2471.
[9] P. Meriaudeau, C. Naccache, Adv. Catal. 44 (2000) 505.
[10] J. Houzvicka, V. Ponec, Catal. Rev.-Sci. Eng. 39 (1997) 319.
[11] M. Guisnet, P. Andy, N.S. Gnep, C. Travers, E. Benazzi, in: H. Chon, S.-K. Ihm, Y.S. Uh (Eds.), Progress in Zeolite and Microporous Materials, in: Stud. Surf. Sci. Catal., vol. 105B, Elsevier, Amsterdam, 1997, p. 1365.
[12] W.-Q. Xu, Y.-G.S. Yin, S.L. Suib, C.-L. O'Young, J. Phys. Chem. 99 (1995) 758.
[13] W.-Q. Xu, Y.-G.S. Yin, S.L. Suib, J.C. Edwards, C.-L. O'Young, J. Phys. Chem. 99 (1995) 9443.
[14] W.-Q. Xu, Y.-G.S. Yin, S.L. Suib, C.-L. O'Young, 210th National Meeting, ACS, Chicago.
[15] J. Houzvicka, S. Hansildaar, J.G. Nienhuis, V. Ponec, Appl. Catal. A 176 (1999) 83.
[16] K.P. de Jong, H.H. Mooiweer, J.G. Buglass, P.K. Maarsen, in: C.H. Bartholomew, G.A. Fuentes (Eds.), Catalyst Deactivation 1997, in: Stud. Surf. Sci. Catal., vol. 111, Elsevier, Amsterdam, 1997, p. 127.
[17] S. van Donk, J.H. Bitter, K.P. de Jong, Appl. Catal. A 212 (2000) 97.
[18] S. van Donk, E. Bus, A. Broersma, J.H. Bitter, K.P. de Jong, Appl. Catal. A 237 (2002) 149.
[19] S. van Donk, E. Bus, A. Broersma, J.H. Bitter, K.P. de Jong, in: R. Aillo, G. Giordano, F. Testa (Eds.), Impact of Zeolites and Other Porous Materials on the New Technologies at the Beginning of the New Millenium, in: Stud. Surf. Sci. Catal., vol. 142, Elsevier, Amsterdam, 2002, p. 573.
[20] S. van Donk, E. Bus, A. Broersma, J.H. Bitter, K.P. de Jong, J. Catal. 212 (2002) 86.
[21] F.C. Meunier, L. Domokos, K. Seshan, J.A. Lercher, J. Catal. 211 (2002) 366.
[22] S.-H. Lee, C.-H. Shin, S.B. Hong, J. Catal. 223 (2004) 200.

[23] P. Andy, N.S. Gnep, M. Guisnet, E. Benazzi, C. Travers, J. Catal. 173 (1998) 322.
[24] P. Andy, D. Martin, M. Guisnet, R.G. Dell, C.E.A. Catlow, J. Phys. Chem. B 104 (2000) 4827.
[25] P. Meriaudeau, R. Bacaud, L. Ngoc Hung, A.T. Vu, J. Mol. Catal. A 110 (1996) L177.
[26] J. Cejka, B. Wichterlova, P. Sar, Appl. Catal. A 179 (1999) 217.
[27] M. Boronat, P. Viruela, A. Corma, J. Phys. Chem. A 102 (1998) 982.
[28] L.M. Petkovic, G. Larsen, J. Catal. 191 (2000) 1.
[29] D.M. Brouwer, Rec. Trav. Chim., Pays-Bas 87 (1968) 1435.
[30] F. Chevalier, M. Guisnet, R. Maurel, in: G.C. Bond, P.B. Wells, F.C. Tompkins (Eds.), in: Proc. 6th Intern. Congr. Catal., vol. 1, The Chemical Society, 1976, p. 478.
[31] H.G. Karge, in: H. van Bekkum, E.M. Flanigen, J.C. Jansen (Eds.), Introduction to Zeolite Science and Practice, in: Stud. Surf. Sci. Catal., vol. 58, Elsevier, Amsterdam, 1991, p. 531.
[32] L. Domokos, L. Sefferts, K. Seshan, J.A. Lercher, J. Mol. Catal. A 162 (2000) 147.
[33] B. Wichterlova, N. Zilkova, E. Uvarova, J. Cejka, P. Sarv, C. Paganini, J.A. Lercher, Appl. Catal. A 182 (1999) 297.
[34] H.S. Cerqueira, P. Ayrault, J. Datka, M. Guisnet, Micropor. Mesopor. Mater. 38 (2000) 197.
[35] D.S. Bystrov, Zeolites 12 (1992) 328.
[36] S. Jolly, J. Saussey, J.C. Lavalley, Catal. Lett. 21 (1994) 141.
[37] M. Guisnet, P. Andy, Y. Boucheffa, N.S. Gnep, C. Travers, E. Benazzi, Catal. Lett. 50 (1998) 159.
[38] R.J. Pellet, D.G. Casey, H.-M. Huang, R.V. Kessler, E.J. Kuhlman, C.-L. O'Young, R.A. Sawicki, J.R. Ugolini, J. Catal. 157 (1995) 423.
[39] P. Canizares, A. Carrero, P. Sanchez, Appl. Catal. A 190 (2000) 93.
[40] Z.R. Finelli, C.A. Querini, R.A. Comelli, Appl. Catal. A 247 (2003) 143.
[41] J. Houzvicka, V. Ponec, Ind. Eng. Chem. Res. 37 (1998) 303.
[42] F. Jousse, L. Leherte, D.P. Vercauteren, Mol. Simulation 17 (1996) 175.
[43] L. Domokos, L. Lefferts, K. Seshan, J.A. Lercher, J. Catal. 203 (2001) 351.
[44] L. Domokos, L. Lefferts, K. Seshan, J.A. Lercher, J. Catal. 197 (2001) 68.
[45] A.W. Peters, W.C. Cheng, M. Shatlock, R.F. Wormsbecher, E.T. Habib, in: D. Barthomeuf, E.G. Derouane, W. Hölderich (Eds.), Guidelines for Mastering the Properties of Molecular Sieves, in: NATO ASI Series, Series B, vol. 221, Plenum Press, New York, 1990, p. 365.
[46] A.G. Stepanov, M.V. Luzgin, S.S. Arzumanov, H. Ernst, D. Freude, J. Catal. 211 (2002) 165.
[47] S. Morin, P. Ayrault, S. El Mouahid, N.S. Gnep, M. Guisnet, Appl. Catal. A 159 (1997) 317.
[48] M. Guisnet, S. Morin, N.S. Gnep, in: C. Song, J.M. Garcés, Y. Sugi (Eds.), Shape-Selective Catalysis, Chemicals Synthesis and Hydrocarbons Processing, in: ACS Symposium Series, vol. 738, ACS, Washington, DC, 1999, p. 334.
[49] M.A. Asensi, A. Martinez, Appl. Catal. A 183 (1999) 155.
[50] D. Rutenbeck, H. Papp, H. Ernst, W. Swieger, Appl. Catal. A 207 (2001) 153.
[51] B. de Ménorval, P. Ayrault, N.S. Gnep, M. Guisnet, Catal. Lett. 94 (2004) 211.
[52] M. Guisnet, P. Magnoux, Appl. Catal. A 212 (2001) 83.